Theoretical study of the effects of solvent environment on photophysical properties and electronic structure of paracyclophane chromophores

Artëm Masunov[a] and Sergei Tretiak
Los Alamos National Laboratory, Theoretical Division and Center for Nonlinear Studies, Los Alamos, New Mexico 87545

Janice W. Hong, Bin Liu, and Guillermo C. Bazan
Department of Chemistry, University of California, Santa Barbara, California 93106

(Received 6 December 2004; accepted 31 January 2005; published online 14 June 2005)

We use first-principles quantum-chemical approaches to study absorption and emission properties of recently synthesized distyrylbenzene (DSB) derivative chromophores and their dimers (two DSB molecules linked through a [2.2]paracyclophane moiety). Several solvent models are applied to model experimentally observed shifts and radiative lifetimes in Stokes nonpolar organic solvents (toluene) and water. The molecular environment is simulated using the implicit solvation models, as well as explicit water molecules and counterions. Calculations show that neither implicit nor explicit solvent models are sufficient to reproduce experimental observations. The contact pair between the chromophore and counterion, on the other hand, is able to reproduce the experimental data when a partial screening effect of the solvent is taken into account. Based on our simulations we suggest two mechanisms for the excited-state lifetime increase in aqueous solutions. These findings may have a number of implications for organic light-emitting devices, electronic functionalities of soluble polymers and molecular fluorescent labels, and their possible applications as biosensors and charge/energy conduits in nanoassemblies. © *2005 American Institute of Physics*.
[DOI: 10.1063/1.1878732]

I. INTRODUCTION

The interest in the molecules studied in this paper is twofold. First, [2.2]paracyclophane (PCP)-based chromophores can serve as a model of intermolecular contacts and solid-state interactions in photoluminescent conducting polymers, widely used in organic light-emitting devices.[1] The PCP core holds two π-conjugated systems cofacially (scheme 1) at a distance that is shorter than the van der Waals distance, and thus provides strong through-space interactions between those systems which can strongly affect the photophysical properties of chromophores and serves as a conduit for delocalization of excitations between chains. Second, water-soluble conjugated oligomers are promising fluorescent labels for biomedical applications.[2] Molecules used for these applications should not be sensitive to environmental perturbations and retain their emission properties and high quantum yield. Detailed experimental studies accompanied by careful theoretical analysis can provide a valuable insight into the nature of underlying fundamental photophysical processes and, ultimately, may help in designing robust novel fluorescent labels.

The electronic structure of unsubstituted PCP was studied theoretically using semiempirical approaches by Canuto and Zerner more than a decade ago.[3] They analyzed the excited states in terms of two weakly interacting π systems. The time-dependent Hartree–Fock technique was then used to study large PCP derivatives with extended π systems.[4] It was found that fluorescent properties of these derivatives, unlike unsubstituted PCP, are strongly dependent on the nature of the lowest excited state. PCP derivatives and related compounds were subject of a large number of subsequent combined experimental and theoretical studies,[5] including their nonlinear optical properties.[6,7]

In particular, the recent experimental investigation[8] of PCP and distyrylbenzene (DSB) derivatives reports that water-soluble ionically derivatized PCP chromophores (PCPnw and PCPdw, see scheme 1) exhibit significant solvatochromic shifts in their emission spectrum (~50 nm) and about 20 ns (i.e., an order of magnitude) longer lifetimes in aqueous solution compared to neutrally derivatized analogs

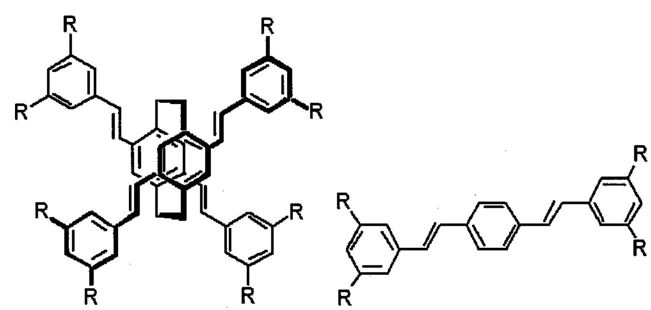

SCHEME 1. Chromophores studied in this work: PCPn ($R{=}CH_2CH_3$), PCPd ($R{=}OCH_3$), PCPnt [$R{=}(CH_2)_6Br$], PCPnw [$R{=}(CH_2)_6NMe_3^+ \cdot Br^-$], PCPdt [$R{=}OSi(CH_3)_2t\mathrm{Bu}$], PCPdw [$R{=}O(CH_2)_4SO_3^- \cdot NBu_4^+$], DSBn ($R{=}CH_2CH_3$), DSBd ($R{=}OCH_3$), DSBnt [$R{=}(CH_2)_6Br$], DSBnw [$R{=}(CH_2)_6NMe_3^+ \cdot Br^-$], DSBdt [$R{=}OSi(CH_3)_2t\mathrm{Bu}$], and DSBdw [$R{=}O(CH_2)_4SO_3^- \cdot NBu_4^+$].

[a]Author to whom correspondence should be addressed. Electronic mail: amasunov@t12.lanl.gov

(PCPnt and PCPdt) in toluene solution. Side-chain functionality was found to have no effect on the excited states of the core-conjugated system, since both ionic and neutral chromophores (PCPdw and PCPdt) have practically indistinguishable photophysical properties, for example, when dissolved in the same solvent [dimethyl sulfoxide (DMSO)]. In the contrast, DSB monomer analogs (see scheme 1) display much less pronounced difference in aqueous versus nonpolar solutions (~5 nm and 1 ns, respectively).

This paper is aimed to elucidate electronic mechanisms leading to these differences. We employ first-principles quantum-chemical calculations and different theoretical models accounting for solvent environment, and report both successes and failures.

II. COMPUTATIONAL DETAILS

All quantum-chemical calculations were performed using the GAUSSIAN03 suite.[9] This package implements a nonequilibrium integral equation formalism polarizable continuum model (IEFPCM),[10] which we utilized in our simulations. Saturated molecular side-chains were truncated (PCPn, PCPd, DSBn, and DSBd, see scheme 1), as they do not participate in the conjugated electronic system. Explicit water molecules and counterions were added in some calculations, as described in Sec. III. Ground-state optimized geometries have been obtained using the Hartree–Fock (HF) theory level combined with the Slater-type orbitals with three Gaussians (STO-3G) basis set. For ground-state geometries, we previously found that HF method is superior to the density-functional theory (DFT) approach based on the hybrid Becke 3 Lee–Yang–Parr (B3LYP) functional by reproducing accurately the bond length alternation parameters in similar conjugated systems when compared to available experimental structures.[1] The molecular geometries of the lowest excited states were optimized at the configuration interaction singles (CIS) / STO-3G theory level. Time-dependent DFT (TD-B3LYP) optimizations for the large conjugated molecules were recently found to be unstable and often converging to unphysical charge-transfer states with vanishing oscillator strengths.[12] The excited-state electronic structures were calculated using the time-dependent DFT (TD-B3LYP) approach,[13] which was found to be accurate for excited states in conjugated molecules,[14] and, in particular, for both linear and nonlinear spectra in centrosymmetrically substituted chromophores.[7,11] At the excited-state optimal geometry, transition frequencies $\Omega_{\rm ge}^{(f)}$ and dipoles $\mu_{\rm ge}^{(f)}$ corresponding to the vertical fluorescence process were used to calculate the approximate radiative lifetime τ_0 as[15] (cgs units)

$$\frac{1}{\tau_0} = \frac{4}{\hbar c^3 (n^2+2)} \Omega_{\rm ge}^{(f)^3} \mu_{\rm ge}^{(f)^2}, \tag{1}$$

where $\hbar\hbar$ is the Plank's constant, c is the speed of light, and n is the refractive index.

To analyze the nature of the excited states involved in the photophysical processes we further used the natural transition orbitals (NTOs) for excited states,[16] derived from the calculated transition densities. This analysis offers the most compact representation of a given transition density in terms of an expansion into single-particle transitions. This approach is particularly attractive for given molecules, since each excited state in question can be well represented as a transition between a single dominant pair of transition orbitals (with 84% or more contribution). Figures of transition orbitals were drawn using the XCRYSDEN graphical package.[17]

III. RESULTS AND DISCUSSION

A. Molecular structures in vacuum

As we pointed out previously,[11] even the most accurate electronic structure method will fail if used with an inaccurate molecular geometry. Therefore, we need to select a theory level, both feasible for routine geometry optimizations, and reliable enough to accurately reproduce the details of the molecular geometry. Two geometric parameters are especially important for the electronic properties of conjugated molecules: planarity which can be defined as dihedral angle along the backbone, and bond length alternation [BLA, or the difference in length between the single and double bonds, $r(\mathrm{C-C}) - r(\mathrm{C{=}C})$]. The molecular planarity for stilbene derivatives was a matter of controversy in the past three decades.[11,18] Apparently, it is determined by the balance of two opposite trends. Conjugation of the π system leads to planarization of the molecule, while steric repulsion between the ethylenic and the *ortho*-hydrogen atoms of the phenyl rings is responsible for the twist along the single bond.

Experimentally, *trans*-stilbene appears to have a large (32°) torsion angle in the gas phase[19] and is considerably more planar (5°) in the crystal.[20] However, various factors, such as ambiguity in averaging over motions with the large amplitude in the gas phase, dynamic disorder (pedaling motion[21]) in crystals, and effects of crystalline environment, complicate the comparison with theoretical values. Indirect experimental evidence for planarity of the free stilbene molecules in solution is obtained from the fact that simulated spectra (both vibrational[22] and electronic[11]) fit much better the experimental data with the assumption of molecular planarity. Studies of the fine rotational structure of the electronic spectra in a collision-free environment in a molecular beam indicate that stilbene is planar in both the ground and first excited states.[23]

Theoretical results for stilbene geometry optimizations were recently reviewed in Ref. 14. Almost all semiempirical and *ab initio* methods predict the planar geometry of stilbene (C_{2h}) to be a saddle point, while the absolute minimum is nonplanar (C_2). In contrast, DFT methods predict the absolute minimum to be planar. In general, many gradient-corrected and hybrid density functionals show very good accuracy for small molecular systems. It is also known that the performances of the same functionals are of a lower level in large conjugated systems, but this defect becomes evident in going towards the limit of an infinite system. Many functionals such as local-density approximation (LDA) and even gradient-corrected versions lead to unphysical behavior of some observables. For example, they do not reproduce excitonic effects. Mixed hybrid methods partially correct these deficiencies.[24] Even though, hybrid B3LYP functional is

TABLE I. Energies (kcal/mol) for the three points on *trans*-stilbene potential energy-surface relative to the planar structure: twisted C_2 (27°), transition state to the rotation of one phenyl group C_s, and second-order saddle point for the simultaneous rotation of both phenyl groups C_{2h}.

	C_2	C_s	C_{2h}
HF/STO-3G	0.85	4.48	8.52
HF/6-31G	−0.17	3.15	7.71
HF/6-31G**	−0.36	2.79	6.63
B3LYP/STO-31G	1.54	6.07	11.38
B3LYP/6-31G	1.10	5.33	9.89
Benchmark[a]	0.24	4.39	9.35

[a]Reference 18.

known to overdelocalize electrons—a feature inherited from the free-electron gas model.[25] Specifically, it significantly overestimates rotation barriers around single bonds,[26] and underestimates BLA values.[27] B3LYP planarity predictions, therefore, should be taken somewhat skeptically. The results may improve when a portion of HF exchange in the hybrid functional increases. One should note that the energy barrier to planarization of stilbene is predicted to be less than 1 kcal/mol at all theory levels. Therefore, the relative stability of the planar versus nonplanar structures still may be reversed after the zero-point vibration energy is taken into account and/or the basis set is increased. Such a reversal was found, for instance, by Masunov and Dannenberg for the urea molecule.[28]

An extrapolation to the infinite basis set limit was recently attempted by Kwasniewski *et al.*[18] In their focal point analysis they used the B3LYP/correlation consistent polarized valence triple zeta (cc-pVTZ) optimized geometry for the minimum (planar structure), saddle points to the rotation of one and both phenyl groups, and artificially twisted C_2 structures as an estimate for the nonplanar geometry. Although the planar geometry was found unstable at the HF limit, account for electron correlation with the Møller–Plesset second-order perturbation theory (MP2) and coupled clusters singles and doubles with triple corrections method [CCSD(T)] makes it an absolute minimum. This suggests that after the large basis set is used and electronic correlation is accounted for, the stilbene molecule is, in fact, planar. Unfortunately, at this level of theory direct geometry optimization is not feasible. Even though the focal point analysis study does not provide direct evidence, it presents the best *ab initio* results to date, and provides three benchmark points on the *trans*-stilbene ground-state potential-energy surface which allow us to select appropriate theory level. We tested several computationally inexpensive theory levels, including those using minimal STO-3G basis set. The minimal basis set sometimes gives surprisingly good results for some molecular properties due to compensation of errors of different types. This compensation, however, does not hold for many other properties, and STO-3G calculations are not reliable without careful comparisons with higher accuracy approaches and experiment. In the present cases the performed checks (presented in Table I) show that HF/STO-3G results to be acceptable for this benchmark set. Incidentally, with the minimal basis set the planar structure is the most stable even at the HF level.

TABLE II. Bond lengths and bond length alternation parameter (BLA, Å) in the central bridge of the stilbene.

Theory level	Symm	R(C═C)	r(C–C)	BLA
AM1	C_2	1.343	1.453	0.110
PM3	C_{2h}	1.342	1.457	0.115
HF/STO-3G	C_{2h}	1.322	1.494	0.172
HF/6-31G	C_{2h}	1.332	1.475	0.143
HF/6-31G	C_2	1.332	1.475	0.143
HF/VZP[a]	C_{2h}	1.332	1.479	0.147
CASSCF(12:10)/VZP[a]	C_{2h}	1.351	1.479	0.128
HF/6-31G**[b]	C_2	1.327	1.478	0.151
MP2/6-31G**	C_2	1.351	1.464	0.113
CCD/6-31G*	C_2	1.345	1.476	0.131
B3LYP/6-31G	C_{2h}	1.357	1.458	0.101
B3LYP/6-31G**[b]	C_{2h}	1.348	1.466	0.118
B3LYP/cc-pVTZ[b]	C_{2h}	1.342	1.463	0.121
B3LYP/cc-pVTZ[b]	C_2	1.341	1.465	0.124
X-ray[c]	C_i	1.326	1.471	0.145
GED[d]	C_2	1.33	1.48	0.15

[a]Reference 29.
[b]Reference 18.
[c]Reference 21.
[d]Reference 19.

Extrapolation of the bond length alternation parameter to the limit of the infinite basis set is unfeasible, but one can observe several trends from the calculated values, summarized in Table II. At the HF/6-31G and HF/6-31G** levels both absolute bond lengths and BLA values are in closest agreement with experiment, and they do not change significantly when the basis set size is increased. At the MP2/6-31G** level the BLA is decreased by 0.04 Å, but half of this decrease is lost when higher-order electron correlations are taken into account at both CCSD and complete active space self-consistent field (CASSCF) levels. At the B3LYP/6-31G** level the BLA is very similar to the values obtained from the MP2, and it somewhat increases with the size of the basis set. One may conclude that both DFT and MP2 overdelocalize double bonds in stilbene and the BLA tends to return to its HF value as the basis set size and the order of electron correlation are increased. This observation supports the use of the HF method for geometry optimizations.

The lowest singlet excited state (S_1) of stilbene is ex-

TABLE III. Calculated and experimental torsional vibrational frequency (cm^{-1}).

Method	Frequency
HF/STO-3G	15
HF/6-31G	43*i*
B3LYP/STO-3G	21
B3LYP/6-31G	12
Experiment, S_0[a]	9
CIS/STO-3G	40
CIS/6-31G	19*i*
Experiment, S_1[a]	35

[a]Reference 31.

pected to have a quinoidal structure, which leads to planarization. There are several spectroscopic evidences confirming the planar structure of S_1, which is more rigid than the ground-state (S_0) structure. In particular, while the electronic absorption spectrum of stilbene has a distinguishable vibronic structure at low temperatures only, the emission spectra retain a vibronic structure even at the room temperature.[30] The rotational spectrum analysis results in a conclusion of planarity for the excited-state S_1 as well.[23] The relative rigidity of the excited state is reflected in a higher frequency of the torsional vibrational mode at the *trans*-stilbene excited state ($35\ \mathrm{cm}^{-1}$ vs $9\ \mathrm{cm}^{-1}$ in the ground state).[31] As one can see from Table III, both ground- and excited-state torsional vibrational frequencies are reproduced well with the minimal basis set again. BLA parameter in the excited state changes sign (−0.042 Å at the CASSCF(12:10)/VZP level). This effect is qualitatively reproduced at the CIS/STO-3G level as well (BLA=−0.007 Å).

After we established that the HF/STO-3G and CIS/STO-3G theory levels for ground and excited states, respectively, are sufficient to reproduce important geometric parameters in the stilbene, they were applied for the geometry optimization of the molecules under study in the ground (S_0) and first singlet excited states (S_1). The conformation of PCP molecules was taken from the crystal structures of analogs, although qualitative comparison of bond lengths and BLA values are not possible due to static disorder (different enantiomers, occupying the same positions in the crystal).[5(f)] The geometry was optimized assuming the highest possible symmetry (C_{2h} for DSB and D_2 for PCP), lower symmetry (C_2 and C_s for DSB and C_2 for PCP), and with no symmetry constraints. Highly symmetric structures were found to be the energy minima for all ground states and for the excited states of DSBn and DSBd. C_2 was found more stable for the excited states of both PCPn (by 18.8 kcal/mol) and PCPd (by 6.2 kcal/mol). The BLA was found to have different values in nonequivalent π systems for S_1 of PCPd (0.173 and 0.087 Å), which are close to S_0 of DSBd (0.174 Å) and S_1 of DSBd (0.080 Å), respectively. Similar values were found for S_1 of PCPn. This already indicates that the relaxation of the excited-state S_1 in PCP molecules leads to localization of the excitation on one of the monomer units. Similar effect was reported previously.[32,33]

B. The nature of absorbing and emitting excited states

Excited states of DSB and PCP molecules were calculated at the TD-B3LYP/6-31G//HF/STO-3G level (in conventional quantum-chemical notation "single point// optimization level"). Table IV shows computed excitation energies of optically active transitions up to four lowest excited states (these correspond to the vertical absorption values), and compares them to the available experimental data taken at the absorption maxima. Overall calculations agree well with experiment, given the uncertainty of the spectral-broadening effects. The respective dominant pairs of NTOs (Ref. 16) for these states are shown in Fig. 1. As expected, DSBn has the only one excited-state S_1 with appreciable oscillator strength. It has essentially a highest occupied molecular orbital (HOMO) to lowest occupied molecular orbital (LUMO) character, which means that the particle/hole NTO pair is heavily dominated by HOMO/LUMO pair. In this case, HOMO describes the distribution of double bonds in a classical Lewis structure, and LUMO corresponds to a quinoid distribution of double bonds. The amplitudes of LUMO are somewhat larger for the central phenyl ring atoms, than for the terminal ones. This effect can be described as partial charge transfer to the central phenyl ring upon excitation.

TABLE IV. Calculated (gas phase) and experimental (toluene, Ref. 8) absorption wavelength λ, calculated oscillator strengths f_{calc}, and experimental relative intensity I_{exp}.

	State	λ_{calc}, nm (eV)	λ_{exp}, nm (eV)	f_{calc}
DSBn	S_1	351 (3.33)	361 (3.43)	1.87
PCPn	S_1	418 (2.96)	397 (2.97)	0.63
	S_2	403 (3.08)	⋯	0.04
	S_3	372 (3.33)	⋯	0.26
	S_4	345 (3.58)	343 (3.62)	1.56
DSBd	S_1	358 (3.46)	361 (3.43)	1.68
PCPd	S_1	426 (2.91)	397 (3.12)	0.54
	S_2	410 (3.02)	⋯	0.03
	S_3	383 (3.23)	⋯	0.24
	S_4	353 (3.51)	338 (3.67)	1.57

Four frontier orbitals of PCPn can be described as symmetric and antisymmetric linear combinations of these monomer HOMOs and LUMOs. They give rise to the first four excited states of PCPn; the corresponding NTOs are shown in Fig. 1. States S_1 and S_4 (symmetric to symmetric and antisymmetric to antisymmetric combinations, respectively) have the largest oscillator strengths. S_2 and S_3 states acquire some oscillator strength as well due to considerable steric distortions. Two monomer branches in PCP strongly interact via both dipolar and through space mechanisms.[4–6] We note that the monomer particle orbitals have increased amplitudes on the central phenyl rings due to the intramonomer charge transfer upon excitation. This leads to a through space delocalization of the particle in the paracyclophane core (as seen in the symmetric combination of the particle NTOs in Fig. 2). The observed energetic splitting between excited states of PCPn strongly depends on the state transition dipoles and, thus, oscillator strengths. We observe significant (∼0.6 eV) splitting between strongly allowed S_1 and S_4 pair and less pronounced (∼0.25 eV) in S_2 and S_3 of PCPn. Compared to S_1 of DSBn, excited states of the dimer PCPn are redshifted which can be attributed to geometric distortion, breaking symmetric split of the excited states in the aggregate around midpoint.[4] Similar trends are observed in the DSBd/PCPd monomer/dimer pair (selected orbitals are shown in Fig. 2).

After the geometry of the excited state relaxes, the monomer units are no longer symmetrically equivalent: both the hole and particle are localized mostly on one of them, in agreement with the BLA values discussed above. Changes in the electronic structure of the excited state upon localization are reflected in the transition orbitals shown in Fig. 2. While

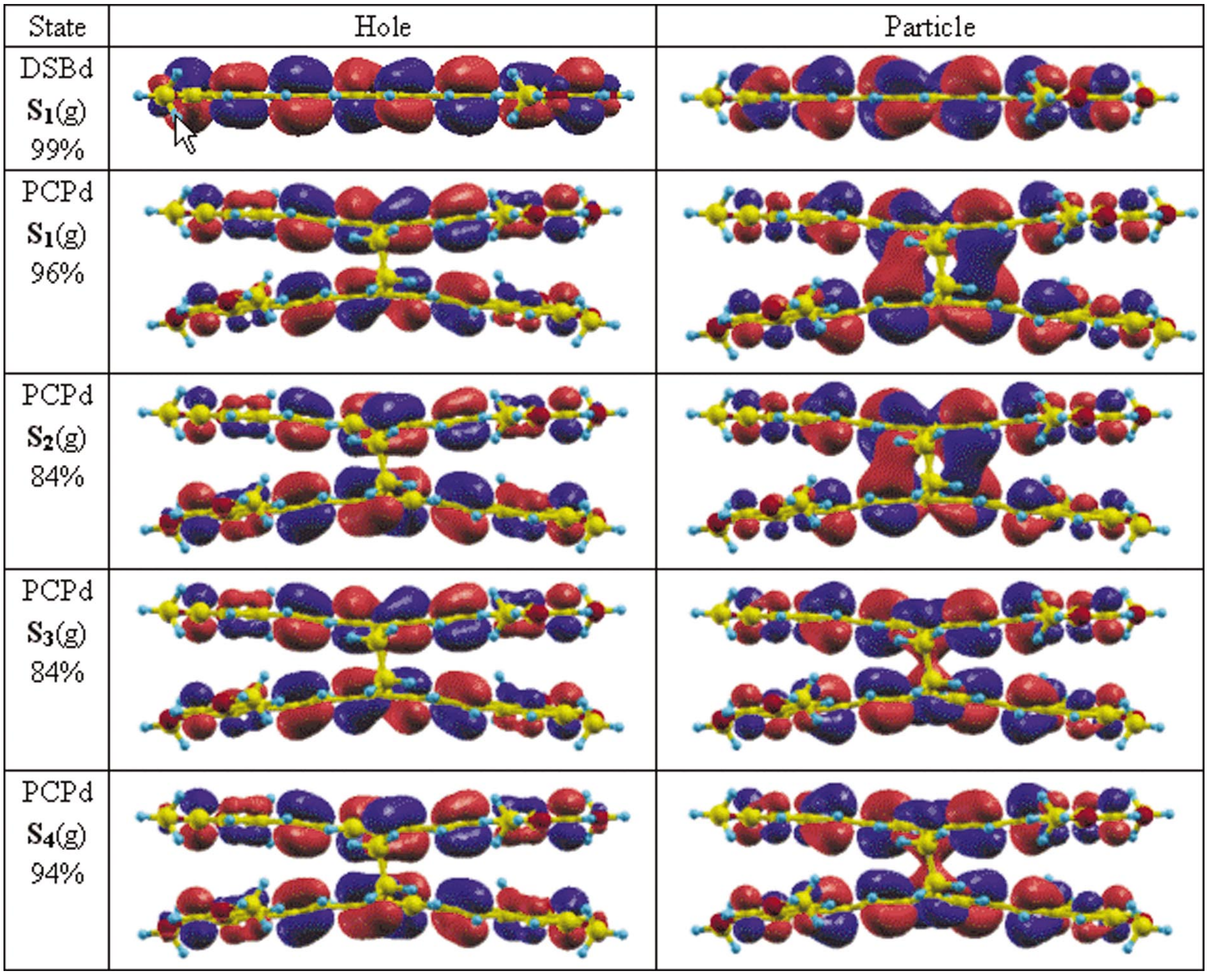

FIG. 1. (Color) Natural transition orbitals of DSBn and PCPn in the ground- (g) state geometry. The percentage indicates a fraction of the NTO pair contribution to a given electronic excitation.

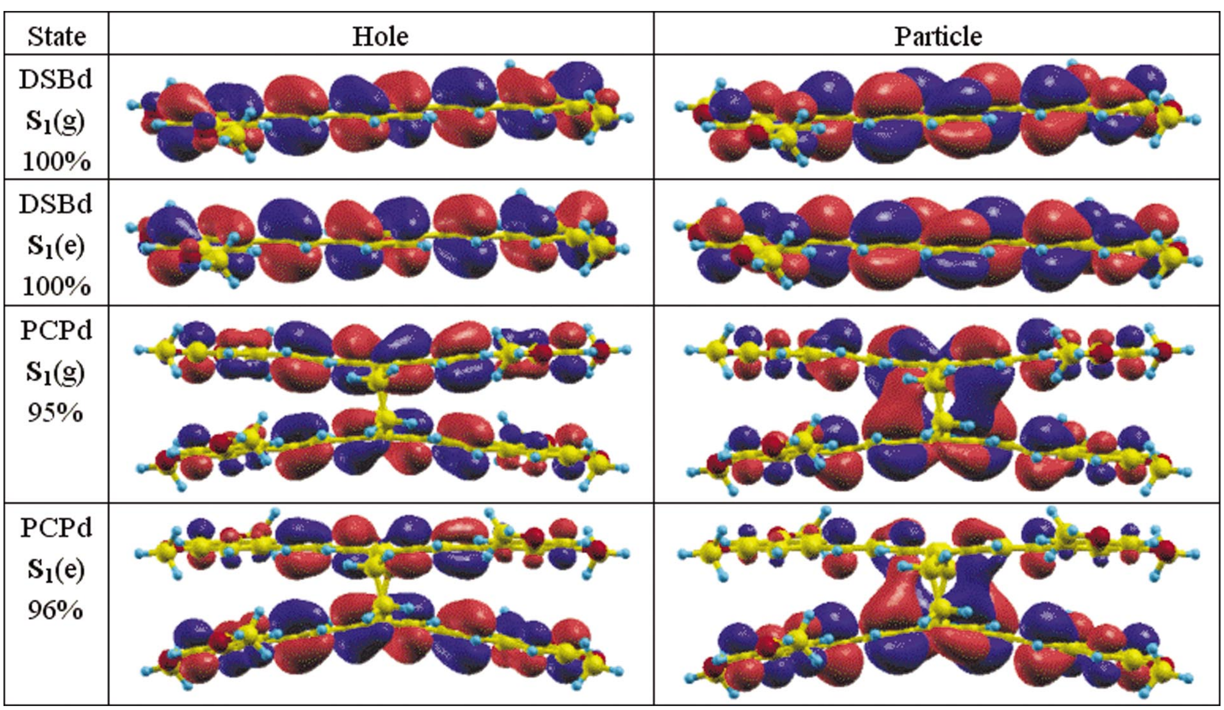

FIG. 2. (Color) Natural transition orbitals for the first excited state of DSBd and PCPd in the ground-(g) and excited- (e) state geometries.

TABLE V. Calculated (gas phase) and experimental (toluene, Ref. 8) fluorescence wavelengths λ and radiative lifetimes τ.

	λ_{calc} (nm) (eV)	λ_{exp} (nm) (eV)	τ_{calc} (ns)	τ_{exp} (ns)
DSBn	428 (2.90)	390 (3.18)	1.0	1.3
PCPn	494 (2.51)	454 (2.73)	3.3	2.9
DSBd	434 (2.86)	391 (3.17)	1.1	1.1
PCPd	493 (2.52)	454 (2.73)	3.7	3.9

neither particle nor hole orbitals of DSB change significantly upon relaxation (apart from the arbitrary sign of the wave function), both hole and especially particle of PCP essentially localize on the bottom monomer. Such localization of the excitation on one of the disjoint-conjugated fragments was previously reported in the theoretical studies[32] and detected experimentally.[32] Comparison of the transition orbitals in Figs. 1 and 2 demonstrates that while *meta*-metoxy substituents somewhat increase involvement of the *para*-carbon atom of the terminal phenyl group in both particle and hole orbitals (inductive effect), lone pairs of the oxygen atoms do not play any appreciable role (no π-resonance effect).

The excitation energies and radiative lifetimes calculated at the optimized geometry of the first excited state are reported in Table V. One can see that the calculated and experimental transition energies agree within 0.3 eV for both the absorption and emission processes, which is typical for TDDFT. The radiative lifetimes for all molecules are in excellent agreement with experiment.

C. Polarizable continuum model and complexes with explicit solvent molecules

The polarizable continuum model (PCM) of solvation is an extension of solvent reaction field models, introduced by Born, Kirkwood, and Onsager for the charge distributions in a spherical cavity surrounded by a dielectric medium.[34] The PCM uses a more realistic shape of the cavity, simulates the dielectric response with discrete charges on the cavity surface, and includes nonpolar contributions to the solvation free energy in addition to the electrostatic component. Various formalisms of PCM have appeared in the literature. They differ in the implementation details, but typically give similar results for neutral molecules. Most of their differences can be attributed to the empirical parameters used (atomic van der Waals radii, etc.). We used integral equation formalism (IEF), which was developed within two alternative formulations.[10,35] These formulations were shown to be equivalent,[36] and only the first one is implemented in the GAUSSIAN03 code.[10] When applied to electronic transitions, the dielectric response is sometimes separated into fast (electronic), and slow (orientational) components with different dielectric constants (nonequilibrium PCM). Here we use nonequilibrium PCM which is introduced[10] in GAUSSIAN03 (Ref. 9) and was reported to increase the solvent effect on the absorption spectra by 8%–10%[35(b)] compared to the single-component model.

Even though the quality of PCM for simulation of solvent effects on NMR, IR, and Raman properties has been established, this method has demonstrated only moderately

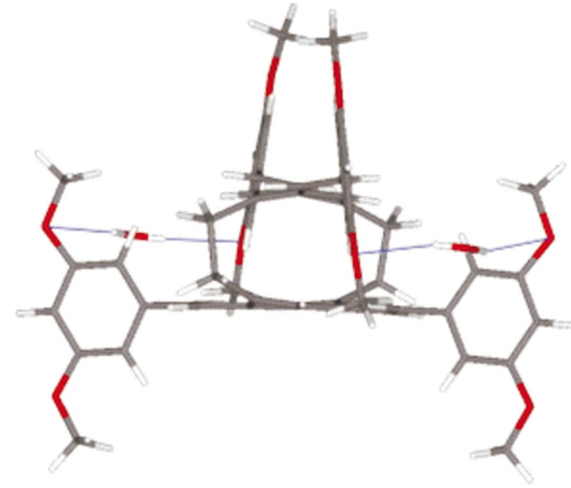

FIG. 3. (Color) Stabilization of PCPd in the twisted conformation by two explicit water molecules (H bonds are shown in blue).

encouraging results when describing solvent effects on the absorption spectra of small polar molecules (pyridazine, pyrimidine, pyrasine,[35(b)] *s*-tetrazine,[37] and formaldehyde[38]). In aprotic (especially, weakly polar) solvents the PCM overestimates solvatochromic shifts from 30% to 300%. In water the PCM alone recovers 30%–50% of the experimental gas/water shifts, and additional explicit water molecules forming H bonds with the solute (at least one for each lone pair) were found necessary to recover the rest.[39] In contrast, for acrolein the PCM quantitatively describes the blue and redshifts in n-π^* and π-π^* excitations, but the addition of explicit water molecules leads to overestimation of these shifts.[40] For nonpolar solutes there is also only qualitative agreement (0.13 eV versus an experimental gas/heptane shit of 0.19 eV for stilbene,[41] and 0.18 versus an experimental penthane/methanol shift of 0.48 eV for methylcyclopropene[42]). Simulations of solvent effects on the fluorescence spectra are scarce, but the available data indicate that PCM is qualitatively correct.[43,44]

Dipolar molecules are known to generate a strong reaction field, and thus the solvent strongly affects their geometry and BLA values.[45] The nonpolar molecules studied here have vanishing dipole moment in the ground state (due to symmetry) and, therefore, they are neither expected to generate a strong solvent response, nor demonstrate large geometric relaxation in a polar solution. Indeed, ground state of PCPd has a vanishing dipole moment by symmetry, and optimization in water using the PCM model yields a structure that is only 0.4 kcal/mol lower in energy, and 0.001 Å different in BLA value. In the excited-state geometry the symmetry is lost, but the dipole moments are rather small (1.2 D in the excited state, and 0.8 D in the ground state) and directed perpendicular to the monomer planes. The change in the BLA value for the excited monomer is somewhat larger (0.005 Å), but the relaxation in the total energy remains almost the same. Not surprisingly, the absorption spectra calculated for the DSBd and PCPd molecules with the PCM model demonstrate negligible shifts relative to the vacuum values. The emission spectra were calculated in the relaxed geometries of the first excited state with the equilibrium PCM (where both compo-

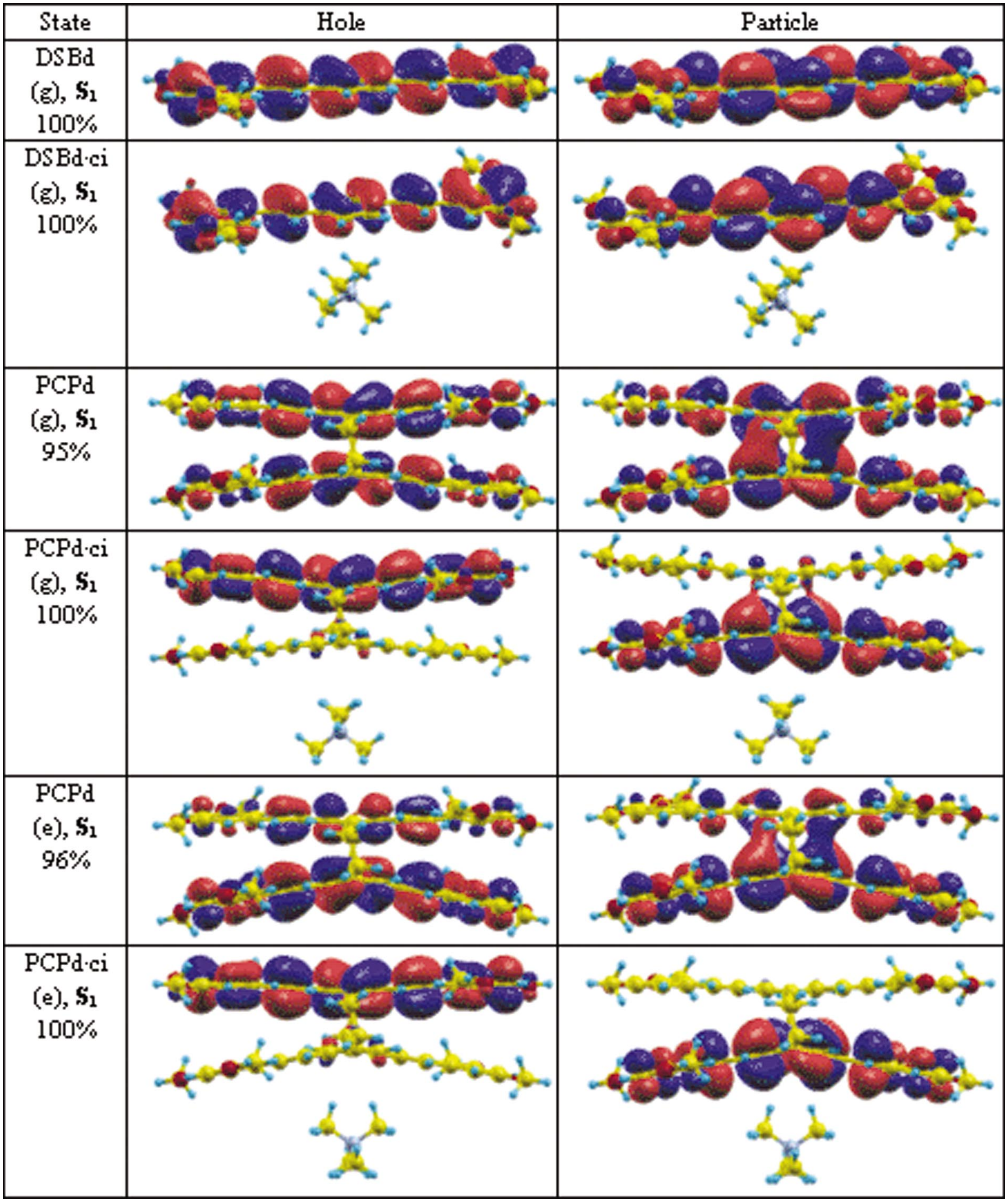

FIG. 4. (Color) Natural transition orbitals for the first excited state of DSBd and PCPd in the ground-(g) and excited- (e) state geometries in vacuum and with counterion at the equilibrium distance.

nents of the reaction field are generated by the charge distribution in this excited state). They demonstrate larger toluene/water shifts (~35 nm), closer to the experiment. However, a 20% decrease in the lifetime is in clear discrepancy with experiment. Similar trends (smaller in values) were obtained for the PCPn molecule.

In order to overcome the limitations of the polarizable continuum model, we built several complexes of PCPd with explicit solvent molecules. Out of several complexes studied, only one of them (Fig. 3) had a significantly longer lifetime for the first excited state. In this complex two water molecules each form two H-bonded bridges between the methoxy sidechains of the different monomers. These bridges are strong enough to stabilize the monomers in the twisted conformation. In the ground state the H-bonding stabilization is 5 kcal/mol at the HF/STO-3G level (vs. 8 kcal/mol for the similar bridges linking methoxy side chains in the planar conformation). The twist of the phenyl groups disrupts π conjugation and leads to the decrease of the transition dipole moment and, subsequently, considerably increases the radia-

TABLE VI. Calculated (counterion complex vs gas phase) and experimental (water vs toluene, Ref. 8) shifts in absorption (Abs.) and photolumenescene (PL) wavelengths λ and respective differences in radiative lifetimes τ.

	PL $\Delta\lambda_{calc}$ (nm)	PL $\Delta\lambda_{exp}$ (nm)	$\Delta\tau_{calc}$, ns	$\Delta\tau_{exp}$, ns	Abs. $\Delta\lambda_{calc}$ (nm)	Abs. $\Delta\lambda_{exp}$ (nm)
DSBn $\cdot Br(H_2)_6^-$	11	18	1.0	1.0	−20	−5
DSBd $\cdot NMe_4^+$	20	24	0.2	0.3	22	−5
PCPn $\cdot Br(H_2O)_6^-$	56	42	12.7	20.6	−7	−5
PCPn $\cdots Br(H_2O)_6^-$	41	42	7.9	20.6	−7	−5
PCPd $\cdot NMe_4^+$	128	57	64.5	29.0	−7	−2
PCPd $\cdots NMe_4^+$	70	57	25.1	29.0	−8	−2

tive lifetime. A similar mechanism is even less possible for PCPn, however, as it has no heteroatoms. Initial geometries of its complexes with water were built in such a way that water molecules formed H bonds ($CH\cdots O$ and $OH\cdots\pi$), and $n\cdots\pi$ donor-acceptor interactions. The excitation energies of these complexes (not shown) were found to be shifted by less than 3 nm, an insignificant shift compared to the toluene/water emission wavelength shifts of ~50 nm, observed in experiment. Nevertheless, such observation of solvent stabilization of conformationally distorted PCP molecules indicates possible existence of an ensemble of solute conformers at the room temperature.

Overall we conclude that both implicit and explicit solvent models fail to reproduce the correct trends, observed in the photoluminescence spectra of PCP chromophores.

D. Complexes with counterions

To understand the nature of the observed experimentally large solvatochromic shifts, one should keep in mind that in order to make the chromophores soluble in a polar solvent, they had been derivatized with ionogenic side chains. Even though the ionic groups are far removed from the π systems and their charge is largely screened out by the solvent, counterions are present in the solvation shells and may form both contact- and solvent-separated complexes with chromophores.

To simulate this possibility, one counterion (NMe_4^+ in the case of DSBd and PCPd, and $Br(H_2O)_6^-$ in the case of DSBn and PCPn) was placed on the twofold axis of the molecule approaching the central ring cofacially. This lowered the symmetry from D_2 to C_2 in the ground state of PCP molecules and made the monomers nonequivalent, similar to the excited-state geometry. The complex of the solute with two ions on the opposite sides of molecule, which would retain D_2 symmetry, seems to be improbable and its simulation was not attempted. Such a complex is presumed to be unstable, unlike solvent-separated complex between ions in aqueous solutions.[46] The main stabilizing factor in the solvent-separated like-charged ion pair is the existence of the bridging water molecules. Such bridges cannot form when the space between ions is occupied by the hydrophobic solute. Therefore, repulsion between the like-charged ions is expected to be strong in aqueous solution.

While optimization in vacuum may describe the solute molecule relatively well, the complex between the chromophore and the ion would require molecular-dynamics simulations with explicit water molecules,[46] which is much more computationally expensive. Instead, we optimized the chromophore-counterion pair (denoted DSB·ci and PCP·ci), and then increased the ion-solute separation by 2 Å (denoted DSB···ci and PCP···ci) to simulate the separation and partial screening effect by the solvent.

The effect of the counterion on electronic structure is illustrated in Fig. 4. In the ground-state geometry of DSBd·ci, the cation decreases the participation of the atomic π orbitals of the central phenyl ring in the hole orbital (repulsion), and increases their participation in the particle orbital (attraction), so that the excitation acquires a character of charge transfer from the terminal to the central phenyl ring. Similar trend is observed in the excited-state geometry (not shown). For PCPd·ci the effect is much more dramatic. Cation completely localizes the electron on the nearest monomer branch, and the hole on the remote branch. Instead of being delocalized between the monomers (in the ground-state geometry), or localized on one monomer (in the excited-state geometry), the excitation almost entirely represents charge transfer from one monomer to another.

The calculated electronic properties of complexes at several geometries are summarized in Table VI. As one can see, both solvatochromic shifts of photoluminescence and increase in the excited-state lifetimes can be well described by the chromophore-ion pair. Addition of $Br(H_2O)_6^-$ ion to DSBn nearly doubles the radiative lifetime and redshifts the photoluminescence maximum by 10 nm in excellent agreement with experiment. Blueshift of the absorption maximum is considerably overestimated. This may indicate that in the ground-state DSBn, ion pair is more spatially separated, so that the electrostatic field of the ion is largely screened off by the solvent environment. The approach of the ion to the chromophore molecule in the excited state is likely to be due to the relatively high polarizability of the chromophore molecule in the excited state, which increases charge-induced dipole attraction. In the case of DSBd $\cdot NMe_4^+$ complex, the opposite charge of the ion increases the partial charge transfer to the central phenyl ring in the excited state. As a result, the redshift instead of the blueshift of the absorption maximum is predicted.

Similar redshifts of the photoluminescence maxima and increase in the radiative lifetimes are observed in the equilibrium structure of PCPn $\cdot Br(H_2O)_6^-$ complex, but the magnitude of both effects is 5–20 times stronger. Such a dramatic effect of the counterion on the radiative lifetime of PCP chromophores compared to that of DSB monomers can be understood using transition orbitals. The approaching ion significantly increases the charge-transfer character of the excitation (from one monomer unit to another). In the charge-transfer state overlap between hole and particle orbitals is small, so that the transition dipole decreases and the lifetime dramatically increases in agreement with experiment. In the case of the PCPd$\cdot$$NMe_4^+$ complex the magnitude of the calculated counterion effects significantly increases, while experimental values increase only slightly. This is likely due to the truncation of the aliphatic chains when the NBu_4^+ ions present in the experiment are replaced with the model NMe_4^+. As a result, optimal chromophore-ion distance is artificially shortened, and enlarged chromophore-ion separation (2 Å versus equilibrium) was found to be a sufficient compensation.

When the PCM was applied to the counterion complexes, the excitation energies and oscillator strengths of the PCP molecules and the corresponding PCP$\cdot$ci complexes showed very little differences (not shown). This may be due to the fact that the solvent around the ion is much more structured than the bulk solvent, and the polarizable continuum model using the bulk dielectric constant fails to reproduce this effect.

IV. CONCLUSIONS

The present theoretical study investigates the absorption and fluorescent properties of PCP-based chromophores shown in scheme 1 in the solvent environment. We use computationally inexpensive *ab initio* approaches to obtain the geometry of the ground and excited states (HF/STO-3G and CIS/STO-3G theory levels, respectively) and show that these methods reproduce important geometric features of similar π-conjugated molecular systems with acceptable accuracy. The time-dependent density-functional theory (at TD-B3LYP/6-31G level) is utilized next to describe excitation energies and radiative lifetimes for transition states. Comparison of the ground- (absorption) and excited- (emission) state geometries and correspondent natural transition orbitals of isolated molecules *in vacuo* reveals that the emitting state is essentially localized on a single monomer branch, whereas the absorbing state remains always delocalized.

To understand possible mechanisms for the strong shifts in the experimentally observed emission maxima and radiative lifetimes in polar versus nonpolar solvents, several solvent models have been tested. Polarizable continuum model is able to reproduce both small solvatochromic wavelength shifts in the absorption spectra, and larger shifts in the fluorescence spectra. However, decrease in the radiative lifetime predicted by PCM disagrees with experiment. The theoretical modeling with explicit solvent shows that water molecules can stabilize the terminal phenyl groups of PCPd in the twisted conformation Fig. 3 by forming hydrogen-bonded bridges between polar substituents on the different monomer branches. However, it leads to the blue solvatochromic shift for PCPd molecules, in contrast to experiment findings. Moreover, this mechanism cannot be applied to PCPn molecules, where absence of oxygen atoms excludes the formation of hydrogen bonds. Thus, neither polarizable continuum model nor explicit water molecules are able to account for experimentally observed behavior.

A possible scenario, which enables us to reproduce closely the experimental data, is the formation of a complex between the chromophore and counterion in a polar solvent. Excited state in these complexes can be described as ion-induced charge transfer. Based on our simulations, the mechanism of the increase in radiative lifetimes of the emitting excited state can be described as follows. In nonpolar solvent, the excitation (both the hole and the particle) is localized on the same branch of PCP chromophore. Increased polarizability of the chromophore in the excited state attracts the nearby ion by charge-induced dipole interaction. The approaching ion then localizes the hole and the particle on the different branches of PCP chromophore, thus decreasing the overlap between them, and, therefore, the transition dipole. In turn this leads to a dramatic increase of the fluorescence lifetimes.[8] A similar unusually large Stokes shift and fivefold increase in the lifetime were recently reported for tetracycline forming complexes with divalent cations.[47]

In the solvents of weaker polarity [such as dimethyl formamide (DMF)], counterions are expected to form contact ion pairs with the charged side chains, rather than with polarizable yet neutral PCP core. The contribution of the ion-induced charge-transfer state will consequently diminish. Therefore, excited-state lifetime in less polar solvents will be similar to that of the neutral derivative, which was indeed observed in experiment.[8] An increase in the radius of counterion by exchange or complexation (for instance, with the crown ether) should lead to a similar result. This can be used as an experimental verification of the proposed mechanism.

The mechanisms described above may have implications on the photophysics of organic molecules and polymers used in organic light-emitting devices and nanoassemblies, as well as soluble conducting polymers used as biosensors. Based on these mechanisms, fluorescent signal from long-lived intermolecular charge-transfer state should decrease if counterions of larger size are used, and increase with ionic strength in the solution. To reduce unspecific wavelength dependence of the biosensor on the polarity of environment, the face of π-electron system should be stericaly protected from the approaching ions.

In organic light-emitting devices (OLEDs), for example, a thin LiF layer was found to improve the efficiency of electron injection from aluminum catode into organic layer of tris-(8-hydroxyquinoline) aluminum (Alq).[48] Several mechanisms of this improvement have been proposed, including formation of ion pairs between Li^+ and Alq anion radicals,[48] and charge-transfer complexes between fluoride anion and Alq.[49] The results of our work suggest that either ion can induce intermolecular charge-transfer complex in a stack of two or more π-conjugated molecules. This indicates the importance of molecular packing and ion intercalation in OLED design.

ACKNOWLEDGMENTS

We wish to thank Dr. Glenn P. Bartholomew for useful discussions, and Dr. Antonio Redondo for his help with the manuscript. The research at UCSB is supported by Mitsubishi Chemical Center for Advanced Materials, and the research at LANL is supported by the Center for Nonlinear Studies, and the LDRD program of the US Department of Energy. This support is gratefully acknowledged (LA-UR-04-7373).

[1](a) M. A. Fox, Acc. Chem. Res. **32**, 201 (1999); (b) G. D. Scholes, J. Phys. Chem. **100**, 18731 (1996).
[2]D. T. McQuade, A. E. Pullen, and T. M. Swagert, Chem. Rev. (Washington, D.C.) **100**, 2537 (2000).
[3](a) S. Canuto and M. C. Zerner, Chem. Phys. Lett. **157**, 353 (1989); (b) S. Canuto and M. Zerner, J. Am. Chem. Soc. **112**, 2114 (1990).
[4](a) G. C. Bazan, W. J. Oldham, Jr., R. J. Lachicotte, S. Tretiak, V. Chernyak, and S. Mukamel, J. Am. Chem. Soc. **120**, 9188 (1998); (b) S. Wang, G. C. Bazan, S. Tretiak, and S. Mukamel, *ibid.* **122**, 1289 (2000); (c) S. Tretiak and S. Mukamel, Chem. Rev. (Washington, D.C.) **102**, 3171 (2002).
[5](a) Y. Morisaki and Y. Chujo, Macromolecules **37**, 4099 (2004); (b) D. S. Seferos, D. A. Banach, N. A. Alcantar, J. N. Israelachvili, and G. C. Bazan, J. Org. Chem. **69**, 1110 (2004); (c) J. Gierschner, H. G. Mack, D. Oelkrug, I. Waldner, and H. Rau, J. Phys. Chem. **108**, 257 (2004); (d) R. Salcedo, N. Mireles, and L. E. Sansores, J. Theor. Comput. Chem. **2**, 171 (2003); (e) L. Guyard, C. Dumas, F. Miomandre, R. Pansu, R. Renault-Meallet, and P. Audebert, New J. Chem. **27**, 1000 (2003); (f) G. P. Bartholomew and G. C. Bazan, J. Am. Chem. Soc. **124**, 5183 (2001); (g) G. P. Bartholomew and G. C. Bazan, Acc. Chem. Res. **34**, 30 (2001); (h) N. Verdal, J. T. Godbout, T. L. Perkins, G. P. Bartholomew, G. C. Bazan, and A. M. Kelley, Chem. Phys. Lett. **320**, 95 (2000); (i) W. J. Warren, Jr., Y.-J. Miao, R. J. Lachicotte, and G. C. Bazan, J. Am. Chem. Soc. **120**, 419 (1998).
[6](a) X. Zhou, A.-M. Ren, J.-K. Feng, and X.-J. Liu, J. Phys. Chem. A **107**, 1850 (2003); (b) G. P. Bartholomew, I. Ledoux, S. Mukamel, G. C. Bazan, and J. Zyss, J. Am. Chem. Soc. **124**, 13480 (2002); (c) J. Zyss, I. Ledoux, S. Volkov, V. Chernyak, S. Mukamel, G. P. Bartholomew, and G. C. Bazan, *ibid.* **122**, 11956 (2000).
[7]G. P. Bartholomew, M. Rumi, S. J. K. Pond, J. W. Perry, S. Tretiak, and G. C. Bazan, J. Am. Chem. Soc. **126**, 11529 (2004).
[8](a) J. W. Hong, B. S. Gaylord, and G. C. Bazan, J. Am. Chem. Soc. **124**, 11868 (2002); (b) J. W. Hong, H. Benmansour, and G. C. Bazan, Chem.-Eur. J. **9**, 3186 (2003); (c) J. W. Hong, H. Y. Woo, B. Liu, and G. C. Bazan, J. Am. Chem. Soc. **127**, 7435 (2005).
[9]M. J. Frisch, G. W. Trucks, H. B. Schlegel *et al.*, GAUSSIAN 03, Revision C.02, Gaussian, Inc., Wallingford, CT, 2004.
[10](a) E. Cances, B. Mennucci, and J. Tomasi, J. Chem. Phys. **107**, 3032 (1997); (b) B. Mennucci, R. Cammi, and J. Tomasi, *ibid.* **109**, 2798 (1998).
[11]A. Masunov and S. Tretiak, J. Phys. Chem. B **108**, 899 (2004).
[12]C. Katan, F. Terenziani, O. Mongin, M. H. V. Werts, L. Porrès, T. Pons, J. Mertz, S. Tretiak, M. Blanchard-Desce, J. Phys. Chem. A **109**, 3024 (2005).
[13](a) E. Runge and E. K. U. Gross, Phys. Rev. Lett. **52**, 997 (1984); (b) M. E. Casida, in *Recent Advances in Density-Functional Methods*, edited by D. A. Chong (World Scientific, Singapore, 1995), Vol. 3.
[14]J. Fabian, L. A. Diaz, G. Seifert, and T. Niehaus, J. Mol. Struct.: THEOCHEM **594**, 41 (2002).
[15]D. A. McQuarrie and J. D. Simon, *Physical Chemistry: A Molecular Approach* (University Science Books, Sausalito, CA, 1997).
[16]R. L. Martin, J. Chem. Phys. **118**, 4775 (2003).
[17]A. Kokalj, J. Mol. Graphics Modell. **17**, 176 (1999); Code available from http://www.xcrysden.org.
[18]S. P. Kwasniewski, L. Claes, J. P. Francois, and M. S. Deleuze, J. Chem. Phys. **118**, 7823 (2003).
[19]M. Traetteberg, E. B. Frantsen, F. C. Mijlhoff, and A. Hoekstra, J. Mol. Struct. **26**, 57 (1975).
[20]J. A. Bouwstra, A. Schouten, and J. Kroon, Acta Crystallogr., Sect. C: Cryst. Struct. Commun. **40**, 428 (1984).
[21]J. Harada and K. Ogawa, J. Am. Chem. Soc. **123**, 10884 (2001).
[22]C. H. Choi and M. Kertesz, J. Phys. Chem. A **101**, 3823 (1997).
[23]B. B. Champagne, J. F. Pfanstiel, D. F. Plusquellic, D. W. Pratt, W. M. Van Herpen, and W. L. Meerts, J. Phys. Chem. **94**, 6 (1990).
[24]S. Tretiak, K. Igumenshchev, and V. Chernyak, Phys. Rev. B **71**, 033201 (2005).
[25]N. Kobko, A. Masunov, and S. Tretiak, Chem. Phys. Lett. **392**, 444 (2004).
[26](a) A. Karpfen, C. H. Choi, and M. Kertesz, J. Phys. Chem. A **101**, 7426 (1997); (b) J. C. Sancho-Garcia, J. L. Bredas, and J. Cornil, Chem. Phys. Lett. **377**, 63 (2003); (c) J. C. Sancho-Garcia and J. Cornil, J. Chem. Phys. **121**, 3096 (2004).
[27]C. H. Choi, M. Kertesz, and A. Karpfen, J. Chem. Phys. **107**, 6712 (1997).
[28]A. Masunov and J. J. Dannenberg, J. Phys. Chem. A **103**, 178 (1999).
[29]V. Molina, M. Merchán, and B. O. Roos, J. Phys. Chem. **101**, 3478 (1997).
[30]J. Gierschner, H. G. Mack, L. Luer, and D. Oelkrug, J. Chem. Phys. **116**, 8596 (2002).
[31]W.-Y. Chiang and J. Laane, J. Chem. Phys. **100**, 8755 (1994).
[32](a) E. Zojer, P. Buchacher, F. Wudl, J. Cornil, J. P. Calbert, J. L. Bredas, and G. Leising, J. Chem. Phys. **113**, 10002 (2000); (b) I. Franco and S. Tretiak, J. Am. Chem. Soc. **126**, 12130 (2004).
[33]D. A. Bussian, M. A. Summers, B. Liu, G. C. Bazan, and S. K. Buratto, Chem. Phys. Lett. **388**, 181 (2004).
[34](a) M. Born, Z. Phys. **1**, 45 (1920); (b) J. G. Kirkwood, J. Chem. Phys. **2**, 351 (1934); (c) L. Onsager, J. Am. Chem. Soc. **58**, 1486 (1936).
[35](a) D. M. Chipman, J. Chem. Phys. **112**, 558 (2000); (b) M. Cossi and V. Barone, *ibid.* **115**, 4708 (2001).
[36]M. A. Aguilar, J. Phys. Chem. A **105**, 10393 (2001).
[37]C. Adamo and V. Barone, Chem. Phys. Lett. **330**, 152 (2000).
[38]C. Zazzaa, L. Bencivenni, A. Grandia, and A. Aschi, J. Mol. Struct.: THEOCHEM **680**, 117 (2004).
[39]F. Aquilante, M. Cossi, O. Crescenzi, G. Scalmani, and V. Barone, Mol. Phys. **101**, 1945 (2003).
[40]F. Aquilante, V. Barone, and B. O. Roos, J. Chem. Phys. **119**, 12323 (2003).
[41]R. Improta, F. Santoro, C. Dietl, E. Papastathopoulos, and G. Gerber, Chem. Phys. Lett. **387**, 509 (2004).
[42]B. Mennucci, J. Tomasi, K. Ruud, and K. V. Mikkelsen, J. Chem. Phys. **117**, 13 (2002).
[43]W. G. Han, T. Q. Liu, F. Himo, A. Toutchkine, D. Bashford, K. M. Hahn, and L. Noodleman, ChemPhysChem **4**, 1084 (2003).
[44]T. Q. Liu, W. G. Han, F. Himo, G. M. Ullmann, D. Bashford, A. Toutchkine, K. M. Hahn, and L. Noodleman, J. Phys. Chem. A **108**, 3545 (2004).
[45]S. Corni, C. Cappelli, M. Del Zoppo, and J. Tomasi, J. Phys. Chem. A **107**, 10261 (2003).
[46]A. Masunov and T. Lazaridis, J. Am. Chem. Soc. **125**, 1722 (2003).
[47]S. Schneider, M. O. Schmitt, G. Brehm, M. Reiher, P. Matousek, and M. Towrie, Photochem. Photobiol. Sci. **2**, 1107 (2003).
[48]M. G. Mason, C. W. Tang, L. S. Hung *et al.*, J. Appl. Phys. **89**, 2756 (2001).
[49]Y. Yuan, D. Grozea, S. Han, and Z. H. Lu, Appl. Phys. Lett. **85**, 4959 (2004).